Journal of Molecular Structure 992 (2011) 27–32

Contents lists available at ScienceDirect

Journal of Molecular Structure

journal homepage: www.elsevier.com/locate/molstruc

Synthesis, characterization, spectroscopic properties, theoretical calculation, and antimicrobial activity of new aryldisulfonamides

Saliha Alyar [a,*], Hüseyin Zengin [b], Neslihan Özbek [c], Nurcan Karacan [d]

[a] Department of Chemistry, Science Faculty, Çankırı Karatekin University, 18100 Çankırı, Turkey
[b] Department of Chemistry, Science and Art Faculty, Gaziantep University, 27310 Gaziantep, Turkey
[c] Department of Primary Education, Faculty of Education, Ahi Evran University, 40100 Kırsehir, Turkey
[d] Department of Chemistry, Science and Art Faculty, Gazi University, 06500 Ankara, Turkey

ARTICLE INFO

Article history:
Received 26 November 2010
Received in revised form 10 February 2011
Accepted 11 February 2011
Available online 17 February 2011

Keywords:
Disulfonamides
Photoluminescence
Antimicrobial activity
TD-DFT/B3LYP calculations
ZINDO/S calculations

ABSTRACT

New aryldisulfonamides were synthesized and characterized by FTIR, ^{1}H NMR, ^{13}C NMR, HETCOR, COSY, LC-MS and elemental analysis techniques. The compounds gave intense emissions, where λ_{max} = 405, 379 and 402 nm, upon irradiation by Ultra-Violet light. The photoluminescence quantum yields and long excited-state lifetimes of the compounds were calculated and were found to have photoluminescence quantum yields 39 ± 1.8%, 45 ± 2.2% and 34 ± 1.4% and long excited-state lifetimes of 3.65 ± 0.16, 4.17 ± 0.20 and 3.15 ± 0.12 ns, respectively. The photoluminescence intensities and quantum yields of compounds varied with the position of substituent on the ring and the chain length between aromatic rings. These novel compounds may be of interest as organic emitting materials for electroluminescent devices. The visible absorption maxima were calculated using time-depended density-functional theory (TD-DFT) and Zerner's intermediate neglect of differential overlap/spectroscopic (ZINDO/S) method in the gas phase. Further, the compounds were evaluated for *in vitro* antimicrobial activity against various microorganisms by microdilution and disk diffusion methods.

1. Introduction

Sulfonamides were the first effective chemotherapeutic agents employed systematically for the prevention and the cure of bacterial infections in humans and other animal systems [1,2]. After the introduction of the penicillin and other antibiotics the popularity of sulfonamides decreased. However they are still used as sulfa drugs such as sulfadiazine, sulfathiazole, sulfamerazine in certain therapeutic fields especially in the case of ophthalmic infections and for urinary and gastrointestinal infections [3,4]. Multidrug resistance (MDR) remains as a significant problem for microbial infection treatments [5–8]. Additionally the threat of bioterrorism using agents such as weaponized *Bacillus anthracis* and *Yersinia pestis* highlight the need for continuing research in infectious diseases and the search for new therapeutic agents [9]. Organic light emitting devices represent an important field of research and has attracted a great deal of attention over recent years [10–12]. For example, organic polymers which exhibit strong luminescence at low driving voltages and in particular those that emit in the blue region are of great interest for flat panel display applications [13,14]. Numerous aromatic amines and polymeric arylamines have also been developed as hole transport layers in organic electroluminescent research [15,16]. The synthesis and fluorescence of N-substituted 1- and 2-aminopyrenes have been studied and their absorption and fluorescence spectra as well as fluorescence quantum yields in different solvents were measured and reported [17]. Their study revealed that the fluorescence quantum yield was dependent on both the structure and solvent polarity. Fluorescent *vic*-dioxime-type ligand and its mono- and dinuclear complexes have been studied [18]. Thus it was noted that the fluorescence spectra of the probe showed a clear shift in excitation wavelength maxima upon metal binding indicating its potential use as ratiometric metal indicator.

In our previous work aliphatic/aromatic disulfonamides and methanesulfonic acid hydrazides/hydrazones were synthesized and tested for antimicrobial and cytotoxic activity [19–26]. Studies herein present the synthesis and characterization of a series of novel disulfonamide derivatives (**1**–**3**) and are shown in Fig. 1. The optical properties of these compounds in solution were also examined. The disulfonamides were found to exhibit photoluminescence, emitting an intense light upon UV irradiation. Further absorption spectra were obtained by semi-empirical ZINDO/S and TD-DFT methods and were compared with experimental data. Antibacterial activities of the synthesized compounds against Gram-positive bacteria (*Staphylococcus aureus* ATCC 25953, *Bacillus*

* Corresponding author. Tel.: +90 376 2181123; fax: +90 376 2181031.
E-mail address: saliha@karatekin.edu.tr (S. Alyar).

0022-2860/$ - see front matter © 2011 Elsevier B.V. All rights reserved.
doi:10.1016/j.molstruc.2011.02.024

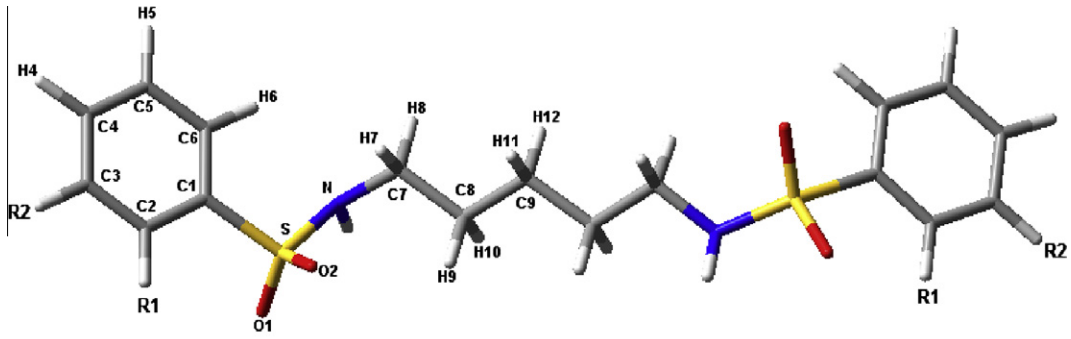

(1) R1= CH_3, R2= H

(2) R1= H, R2= CH_3

(3) R1= CH_3, R2= H

Fig. 1. The chemical structures and labels of atoms for disulfonamides (**1**–**3**).

cereus ATCC 6633 and *Bacillus megaterium* RSKK 5117) and Gram-negative bacteria (*Escherichia coli* ATCC 11230 and *Salmonella enteritidis* ATCC 13076) were evaluated by disk diffusion and microdilution methods.

2. Experimental procedure

2.1. Materials and instrumentation

The elemental analyses (C, H, N and S) were performed on a LECO CHNS 9320 type elemental analyzer. The IR spectra (4000–400 cm^{-1}) were recorded on a Mattson 1000 FT-IR Spectrophotometer with samples prepared as KBr pellets. NMR spectra were recorded on a Bruker-Spectrospin Avance DPX-400 Ultra–Shield (400 MHz) using DMSO as the solvent with TMS as the internal standard. LC/MS-APCl was recorded on an AGILENT 1100 Spectrometer. The melting points were measured using an Opti Melt apparatus. TLC was conducted on 0.25 mm silica gel plates (60F 254, Merck). All solvents were purchased from Merck and reagents were obtained from Aldrich Chem. Co. (ACS grade) and used as received. The single-photon fluorescence spectra of the compounds were collected on a PerkinElmer LS55 Luminescence Spectrometer. All the samples were prepared in spectrophotometric grade tetrahydrofuran (THF) and analyzed in a 1 cm optical path quartz cuvette. The solution concentration of the compounds in THF was 1.0×10^{-5} mol L^{-1} and the samples were excited at 249 nm wavelength. The photoluminescence quantum efficiencies of the compounds calculated using 9.10-diphenylantracene as the standard [27–29].

2.2. General procedure for the synthesis

Nucleophilic substitution reaction of the aromatic diamines with arylsulfonyl chlorides were carried out as follows: THF solution of aromatic diamines were added slowly to THF solutions of the sulfonyl chlorides at −5 °C. The reaction mixture was stirred for 24 h at room temperature and completion of the reaction was monitored by TLC. After the completion of the reaction, the solvent was evaporated in vacuo. The solid residue was purified by column chromatography.

2.2.1. Synthesis of N,N′-butanediyl-bis-2-methylbenzenesulfonamide (1)

Using the general procedure described above from 4.06 mL (0.08 mol) 1,4-diamino butane and 2-methylbenzenesulphonyl chloride 3.85 mL (0.04 mol) a white solid was obtained. The product was filtered and recrystallized from a ethanol/n-hexane (4/1) mixture and was dried *in vacuuo* and stored under ethanol vapor: Yield 78%; mp 183–184 °C; IR (KBr) cm^{-1}: 3281 υ(NH), 1452 δ(NH), 2979 $\upsilon(CH_3)$, 1317 $\upsilon_{asym.}(SO_2)$, 1169 $\upsilon_{sym.}(SO_2)$; Anal. Calcd. for $C_{18}H_{24}N_2O_4S_2$: C, 54.52; H, 6.10; N, 7.06; S, 16.17, Found: C, 54.47; H, 6.00; N, 7.05; S, 16.10.

2.2.2. Synthesis of N,N′-butanediyl-bis-3-methylbenzenesulfonamide (2)

Using the general procedure described above from 4.06 mL (0.08 mol) 1,4-diamino butane and 3-methylbenzenesulphonyl chloride 3.85 mL (0.04 mol) a white solid was obtained. The product was filtered and recrystallized from a ethanol/n-hexane (4/1) mixture and was dried *in vacuo* and stored under ethanol vapor: Yield 80%; mp 183–184 °C; IR (KBr) cm^{-1}: 3294 υ(NH), 1439 δ(NH), 2947 $\upsilon(CH_3)$, 1323 $\upsilon_{asym.}(SO_2)$, 1169 $\upsilon_{sym.}(SO_2)$; Anal. Calcd. for $C_{18}H_{24}N_2O_4S_2$: C, 54.52; H, 6.10; N, 7.06; S, 16.17, Found: C, 54.51; H, 6.00; N, 7.00; S, 15.99.

2.2.3. Synthesis of N,N′-pentanediyl-bis-2-methylbenzenesulfonamide (3)

Using the general procedure described above from 4.06 mL (0.08 mol) 1,5-diamino pentane and 2-methylbenzenesulphonyl chloride 3.85 mL (0.04 mol) a white solid was obtained. The product was filtered and recrystallized from a ethanol/n-hexane (4/1) mixture and was dried *in vacuo* and stored under ethanol vapor: Yield 80%; mp 183–184 °C; IR (KBr) cm^{-1}: 3294 υ(NH), 1439 δ(NH), 2947 $\upsilon(CH_3)$, 1323 $\upsilon_{asym.}(SO_2)$, 1169 $\upsilon_{sym.}(SO_2)$; Anal. Calcd. for $C_{18}H_{24}N_2O_4S_2$: C, 54.52; H, 6.10; N, 7.06; S, 16.17, Found: C, 54.51; H, 6.00; N, 7.00; S, 15.99.

2.3. Structure optimizations

All calculations were performed using a Pentium IV computer with default convergence criteria and Gaussian 03 software package [30]. An extensive search for low energy conformations on potential energy surfaces (PES) of compounds were carried out by using a systematic search with RHF/6-31G(d,p) levels. Minimum energy conformations were re-optimized at DFT/B3LYP/6-311+G(d,p) levels without symmetry constraints. Vibration frequencies calculated ascertain the structure to be stable (no imaginary frequencies).

2.4. Micro dilution assays

E. coli ATCC 11230, *S. enteritidis* ATCC 13076, *S. aureus* ATCC 25923, *B. cereus* ATCC 6633 and *B. magaterium* RSKK 5117 cultures were obtained from the Department of Biology at Gazi University and the Refik Saydam Hygiene Center Culture Collection. Bacterial strains were cultured overnight at 37 °C in Nutrient Broth. These stock cultures were stored in the dark at 4 °C during the survey.

All tests were performed in a Nutrient Broth supplemented with DMSO to a final concentration of 10% (v/v) to enhance their solubility. Test strains were suspended in the Nutrient Broth by adjusting to the 0.5 McFarland standard. The compounds to be tested were dissolved in DMSO to give the highest concentration (450 μg mL^{-1}), and serial dilutions thereafter in sterile 10 mL test tubes containing nutrient broth to give sample concentrations of the range 45–450 μg mL^{-1}. The minimum inhibitory concentration (MIC) values of compounds were determined using a modification of the microwell dilution assay method. 96 well plates were prepared by dispensing 95 μL of nutrient broth and 5 μL of the inoculums into each well. 100 μL from test compounds initially prepared at 450 μg mL^{-1} concentration were added into the first wells. Then, 100 μL from the serial dilutions was transferred into fourteen consecutive wells. The contents of the wells were mixed and the microplates were incubated at 37 °C for 24 h. The compounds were tested against each microorganisms twice. The MIC values were determined from visual examinations as the lowest concentration of the extracts in the wells with no bacterial growth [31].

2.5. Disc diffusion method

Bacterial susceptibility testing was performed by the disc diffusion method according to the guidelines of Clinical and Laboratory Standards Institute (CLSI) [32]. The sterilized (autoclaved at 120 °C for 30 min), liquefied Mueller Hinton agar (40–50 °C) was inoculated with the suspension of the microorganism (matched to 0.5 McFarland) and poured into a Petri dish to give a depth of 3–4 mm. The paper discs impregnated with the test compounds (60 μg) were placed on the solidified medium. Discs were placed on agar plates and the cultures were incubated at 37 °C for 24 h for bacteria. Inhibition zones formed on the medium were evaluated in mm. Ciprofloxacin (5 μg/disk) was chosen as a standard in antibacterial activity measurements (positive control). DMSO poured disk was used as negative control.

3. Results and discussion

3.1. Structure analysis

NMR spectra of compounds were recorded in DMSO-d_6 and $CDCl_3$ using TMS as the internal standard. ^1H NMR and ^{13}C NMR data for half of the compounds are given in Tables 1 and 2, respectively. It is known that symmetric C and H atoms in the compounds show the same chemical shift due to them having same chemical environment. ^1H NMR spectrum of (**1**) was obtained using DMSO-d_6. In NMR spectra, aromatic proton peaks were observed at about 7.77–7.33 ppm. The chemical shift of the NH group the compound in d_6-DMSO is in the range of 7.59 ppm however in $CDCl_3$ it is at about 4.48 ppm. Difference of chemical shift may be attributed to the formation of intermolecular interactions with the polar solvent DMSO.

The ^{13}C NMR spectrum of (**1**) was obtained using DMSO-d_6. Molecule (**1**) has three different aliphatic carbon atoms and six aromatic carbon atoms. Magnetic shielding constants of C7 and C8 atoms were observed at 41.73 ppm and 26.24 ppm, respectively. Magnetic shielding constants of C7 atom were found to be lower than the chemical shift value of C8 atom. Aromatic carbon peaks are shown to be at about 126.07–138.71 ppm.

The 2D COSY NMR spectrum of (**1**) was obtained using DMSO-d_6. The COSY spectrum confirms the above ^1H spectral assignments. The multiplet at δ 1.30 ppm is for the H_{9-10} protons. In the COSY spectrum horizontal and vertical lines drawn from at δ 1.30 ppm met the off – diagonal peak at 2.68 ppm which was assigned to the H_{7-8} protons. Similarly the lines from the peak at 2.68 ppm met the off-diagonal peak at 1.30 ppm. This establishes the fact that the protons at H_{9-10} split the peak of H_{7-8} protons into multiple and vice versa because they are neighboring protons. From 2D HETCOR NMR spectrum (Fig. 3), it is clear that the peaks at δ values 138.71 and 136.42 in the ^{13}C NMR spectrum did not show any contour in HETCOR confirming that they are non protonated and are assigned to C1 and C2. The correlations between C7–H_{7-8}, C8–H_{9-10} in the zigzag structure and C3–H_3, C4–H_4, C5–H_5, C6–H_6 in the aromatic ring are also observed in HETCOR spectrum.

The IR spectra of the compounds were found to be very similar to each other. More characteristic vibrations of the compound **(1)** is as follows: asymmetric and symmetric stretching vibrations of SO_2 groups were observed at about 1317 and 1169 cm^{-1}, respectively. Terminal methyl stretching vibrations were noted at 2979 cm^{-1}. The presence of single and strong NH band at about 3281 cm^{-1} confirms the presence of secondary amine group in the compound.

3.2. Fluorescence measurements

The optical properties of the compounds (**1**–**3**) were explored using UV–Vis and PL. Absorption and photoluminescence spectra were studied for solutions of compounds (**1**–**3**), excited at 249 nm. The most striking feature was that these compounds gave an intense emission upon irradiation by UV light. The photoluminescence spectrum of (**1**) in THF is shown in Fig. 2. Maximum luminescent intensity was observed at 405 nm and the full width at half maximum was 121 nm. Compound (**1**) exhibited a photolumines-

Table 1
^1H NMR data for compounds (**1**–**3**).

Assignment	(1)		(2)		(3)	
	DMSO	$CDCl_3$	DMSO	$CDCl_3$	DMSO	$CDCl_3$
2-C**H$_3$**	2.60 (s, 3H)	2.65 (s, 3H)	–	–	2.57 (s, 3H)	2.64 (s, 3H)
3-C**H$_3$**	–	–	2.35 (s, 3H)	2.45 (s, 3H)	–	–
H$_7$–H$_8$	2.68 (t, 2H)	2.92 (t, 2H)	2.50 (t, 2H)	2.96 (t, 2H)	2.68 (t, 2H)	2.89 (t, 2H)
H$_9$–H$_{10}$	1.30 (t, 2H)	1.51 (p, 2H)	1.32 (q, 2H)	1.54 (q, 2H)	1.25 (p, 2H)	1.41 (p, 2H)
H$_{11}$–H$_{12}$	–	–	–	–	1.12 (p, 2H)	1.29 (p, 2H)
H$_6$	7.77 (d, H)	7.96 (d, H)	7.45 (d, H)	7.42 (d, H)	7.81 (d, H)	7.95 (d, H)
H$_4$	7.49 (t, H)	7.48 (t, H)	7.45 (d, H)	7.42 (d, H)	7.48 (t, H)	7.46 (t, H)
H$_3$	7.33 (t, 2H)	7.33 (t, 2H)	–	–	7.36 (t, 2H)	7.31 (t, H)
H$_5$	7.33 (t, 2H)	7.33 (t, 2H)	7.49 (t, H)	7.65 (t, H)	7.36 (t, 2H)	7.31 (t, H)
H$_2$	–	–	7.52 (s, H)	7.68 (s, H)	–	–
N**H**	7.59	4.48	7.50	4.58	7.56	4.94

Table 2
^{13}C NMR data for compounds (**1**–**3**).

Assignment	(**1**)	(**2**)	(**3**)
2-**C**H$_3$	19.75	–	19.75
3-**C**H$_3$	–	20.80	–
C7	41.73	42.03	42.06
C8	26.24	26.17	28.53
C9	–	–	22.99
C1	138.71	140.42	138.82
C2	136.42	126.63	136.41
C4	132.40	132.82	132.38
C5	132.22	123.55	132.20
C6	128.30	128.96	128.31
C3	126.07	138.79	126.77

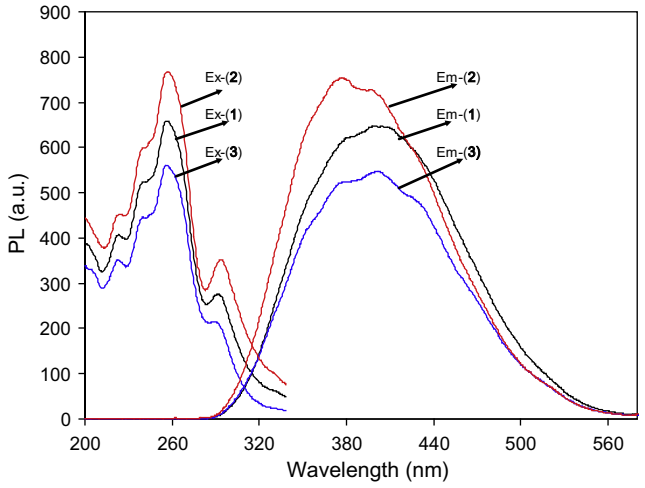

Fig. 2. Photoluminescence spectra of compounds (**1**–**3**) in THF; samples were excited at 249 nm.

cence quantum yield of 39 ± 1.8% and a long excited-state lifetime of 3.65 ± 0.16 ns. The reason for the high quantum yields is that the π-electrons extensive delocalizations form in the chemical structure. Fig. 2 also shows the comparison of excitation and emission spectra of compounds (**1**–**3**) in the solvent THF. The photoluminescence intensities and quantum yields of the compounds varied with the position of the substituent on the ring and the chain length between the aromatic rings. The photoluminescence spectrum of compound (**2**) in THF is also shown in Fig. 2. Maximum luminescent intensity was observed at 379 nm and the full width at half maximum was 126 nm. Compound (**2**) exhibited a photoluminescence quantum yield of 45 ± 2.2% and a long excited-state lifetime of 4.17 ± 0.20 ns. The reason for the high quantum yields is due to the resulting π-electrons extensive delocalizations in the chemical structure of the compound. It can be seen in Fig. 2 that the maximum photoluminescence peak shifted to lower wavelength from 405 to 379 nm with the position of substituent on the aromatic rings. Also, the shoulder peak at 296 on the excitation spectrum becomes more intense and obvious. This emission wavelength difference may be used for tuning properties in photoluminescent devices. As seen in Fig. 2 for compound (**3**) maximum luminescent intensity was observed at 402 nm and the full width at half maximum was 114 nm. Compound (**3**) exhibited a photoluminescence quantum yield of 34 ± 1.4% and a long excited-state lifetime of 3.15 ± 0.12 ns. The maximum luminescent intensity reduced and shifted to lower wavelength for longer chain length between the aromatic rings. The photoluminescence data for the compounds are summarized in Table 3. The quantum yields and excited-state lifetimes of each compound was measured four times, and the results were averaged. Table 3 gives the quantum yields and excited-state lifetimes with their corresponding average deviations among the four results. The deviations give an indication of the reliability of the measurements. The average deviations of quantum yields and lifetimes for all the compounds were less than 5%. The photoluminescent properties of these compounds may indicate great potential for numerous optical and electronic applications.

3.3. UV–Vis spectra

The UV–Vis spectra were calculated using TD-DFT and Zerner's intermediate neglect of differential overlap/spectroscopic (ZINDO/S) methods. TD-DFT calculations were performed in the gas phase. In the calculation of excited energies for the disulfonamides using the B3LYP function, and the 6-31G(d,p), 6-31G+(d,p), 6-311G(d,p) and 6-311+G(d,p) basis sets. The calculated maximum absorption wavelengths and oscillator strengths are given in Table 4. For compounds (**1**) and (**3**), λ_{max} values were 234 nm [6-31G(d,p)], 239 nm [6-31+G(d,p)], 237 nm [6-311G(d,p)] and 240 nm [6-311+G(d,p)]. For compound (**2**), these values are 237, 242, 240 and 243 nm. The results which obtained using the B3LYP function and 6-

Table 3
Photoluminescence data for compounds (**1**–**3**).

Compound	λ_{max} Ex (nm)	In Ex	λ_{max} Em (nm)	In Em	ϕ_f (%)	τ_f (ns)
(**1**)	259 (226;242;295)	652	405 (356;383;434)	645	39 ± 1.8	3.65 ± 0.16
(**2**)	260 (225;241;296)	759	379 (356;401;432)	751	45 ± 2.2	4.17 ± 0.20
(**3**)	259 (225;241;393)	554	402 (354;378;431)	546	34 ± 1.4	3.15 ± 0.12

λ_{max} Ex: maximum excitation wavelength; In Ex: maximum excitation intensity.
λ_{max} Em: maximum emission wavelength; In Em: maximum emission intensity.
ϕ_f: quantum yield; τ_f: excited-state lifetime.

Table 4
Calculated absorption maxima and oscillator strengths for compounds (**1**–**3**).[a]

Compound	DFT/B3LYP					
	Exp[b] λ_{max} (nm)	ZNDO/S	6-31G(d,p)	6-31+G(d,p)	6-311G(d,p)	6–311+G(d,p)
(**1**)	244	273.65 (0.0646)	234.49 (0.0142)	239.15 (0.0164)	237.62 (0.010)	240.36 (0.0159)
(**2**)	252	271.88 (0.0273)	237.13 (0.0178)	242.66 (0.0209)	240.75 (0.0205)	243.97 (0.0211)
(**3**)	244	273.7 (0.1012)	234.39 (0.0140)	239.1 (0.0164)	237.53 (0.0148)	240.3 (0.0158)

[a] Oscillator strengths are given in parenthesis.
[b] In DMSO.

Table 5
Antimicrobial activity of compounds (**1**–**3**) with microdilution method.

Compound	MIC (μg mL^{-1})				
	E. coli ATCC 11230	*S. enteritidis* ATCC 13076	*B. megaterium* RSKK 5117	*B. cereus* ATCC 6633	*S. aureus* ATCC 25953
(1)	90	125	360	125	112
(2)	112	157	380	157	134
(3)	180	300	430	310	250

Table 6
Result of the antimicrobial test of compounds (**1**–**3**); disk potency 60 μg.

Compound	Diameter of inhibition zone (mm)				
	E. coli ATCC 11230	*S. enteritidis* ATCC 13076	*B. megaterium* RSKK 5117	*B. cereus* ATCC 6633	*S. aureus* ATCC 25953
(1)	22	14	–	16	18
(2)	20	13	–	14	15
(3)	14	11	–	11	10
Ciprofloxacin (5 μg/disk)	38	31	15	27	29

311+G(d,p) basis set showed excellent agreement between the experimental and calculated values of λ_{max}. The λ_{max} value obtained with semi-empirical ZINDO/S for the compounds were higher than those obtained using the TD-DFT method. The length of the carbon chain does not change the λ_{max} of compounds. The λ_{max} of the compounds varies with the position of substituent on the ring. The *meta* position of λ_{max} order of aromatic disulfonamides is greater than *ortho*.

3.4. Antibacterial activity

Synthesized compounds (**1**–**3**) were screened for antibacterial activity against Gram-positive bacteria *(S. aureus* ATCC 25923, *B. cereus* ATCC 6633 and *B. megaterium* RSKK 5117) and Gram-negative bacteria (*E. coli* ATCC 11230 and *S. enteritidis* ATCC 13076) by disk diffusion and microdilution methods. The antibacterial activity results are given in Tables 5 and 6. Results indicated that the synthesized compounds possessed a broad spectrum of activity against the tested microorganisms and showed relatively better activity against Gram-negative than Gram- positive bacteria.

Compound (**1**) showed the highest activity with lowest MIC values, 90 μg mL^{-1}, 125 μg mL^{-1} against Gram-negative bacteria *E. coli* and *S. enteritidis*, respectively. All compounds showed poor activity against *B. magaterium,* and compound (**3**) exhibited the lowest inhibitory activity with a MIC of 430 μg mL^{-1}. Among the compounds, compound (**3**) showed the lowest activity against all test microorganisms. The results obtained revealed that the antibacterial activity decreased as the length of the carbon chain increased. However, aromatic disulfonamide compounds showed decrease in antibacterial activity than sulfonyl hydrazide [19]. The primary amine group plays a more important role than secondary amine groups. Furthermore, antibacterial activity of aromatic disulfonamide compounds are higher than aliphatic disulfonamides and sulfonyl hydrazones published in the literature [19,25,33,34]. Compared to reference discs (ciprofloxacin 5 μg/disk), compound (**1**) showed greater activity against *E. coli*. As shown in Table 5 all tested compounds, although applied in 12-fold higher concentrations (60 μg) than the reference ciprofloxacin (5 μg) displayed weak activity against bacteria. The activity order of aromatic disulfonamides is as follows: *ortho* > *meta*; the λ_{max} Ex (nm) and UV–Vis λ_{max} order is: *meta* > *ortho*.

4. Conclusions

Three aromatic disulfonamide derivatives (**1**–**3**) were synthesized and characterized by FT-IR, ^{1}H NMR, ^{13}C NMR, HETCOR, LC-MS and elemental analysis techniques. Compounds (**1**–**3**) were found to exhibit intense photoluminescence at 405, 402 and 379 nm, respectively and the photoluminescence intensities and quantum yields of the compounds varied with the position of substituent on the ring and the chain length between the aromatic rings. These compounds are interesting materials for applications in electroluminescent devices. The TD-DFT calculations were performed using the B3LYP functional with the four different basis sets 6-31G(d,p), 6-31+G(d,p) 6-311 G(d,p) and 6-311+G(d,p) and yielded accurate results for the aromatic disulfonamides. The results obtained using the B3LYP functional showed an excellent agreement between the experimental and calculated values of λ_{max}. Compounds showed broad spectrum antimicrobial activity, and activity decreased as the length of the carbon chain increased. Compound (**1**) showed the best activity with the lowest MIC (420 μg mL^{-1}) against *E. coli* bacteria.

Acknowledgments

The authors wish to thank TUBITAK for the financial support (TBAG 104 T 390 and (MAG 104M 367) and Gazi University Scientific Research Project (05/2008-05). We would also like to thank the Departments of Chemistry at Gazi University and Gaziantep University.

Appendix A. Supplementary material

Supplementary data associated with this article can be found, in the online version, at doi:10.1016/j.molstruc.2011.02.024.

References

[1] A. Bult, in: H. Sigel (Ed.), Metal Ions in Biological Systems, vol. 16, Marcel Decter, New York, 1983, p. 261.
[2] Th. Nogrady, Medicinal Chemistry, second ed., Oxford University press, New York, 1988, p. 383.
[3] E.R. Barnhart (Ed.), Physician s Desk Reference, PDR, 43rd ed., Medical Economics, New York, 1989.
[4] H. Singh, V.K. Srivastava, S.N. Shukla, M.K. Srivastava, M.K. Upadhyay, Indian J. Chem. 33A (1994) 350.
[5] K.A. Metwally, L.M. Abdel-Aziz, E.M. Lashine, M.I. Husseiny, R.H. Badawy, Bioorgan. Med. Chem. 14 (2006) 8675.
[6] N. Hadj-esfandiari, L. Navidpour, H. Shadnia, M. Amini, N. Samadi, M.A. Faramarzi, A. Shafiee, Bioorg. Med. Chem. Lett. 17 (2007) 6354.
[7] M.W. Khan, M.J. Alam, M.A. Rashid, R. Chowdhury, Bioorg. Med. Chem. 13 (2005) 4796.
[8] Z. Nilo, S.H. Alves, H.S. Coelho, D.M. Borchhardt, P. Machado, K.M. Flores, F.M. da Silva, T.B. Spader, J.M. Santurio, H.G. Bonacorso, M.A. Martins, Bioorgan. Med. Chem. 15 (2007) 1947.
[9] R.A. Greenfield, M.S. Bronze, Drug Discovery 8 (2003) 881.
[10] T.R. Chen, J.D. Chen, T.C. Keng, J.C. Wang, Tetrahedron Lett. 42 (44) (2001) 7915.
[11] L. Akcelrud, Prog. Polym. Sci. 28 (2003) 875.

[12] H. Wang, N. Song, H. Li, Y. Li, X. Li, Synth. Met. 151 (2005) 279.
[13] M. Carrard, S. Goncalves-Conto, L. Si-Ahmed, D. Ades, A. Siove, Thin Solid Films 352 (1–2) (1999) 189.
[14] L. Feng, Z. Chen, Polymer 46 (2005) 3952.
[15] C.H. Chen, J. Shi, C.W. Tang, Macromol. Symp. 125 (1998) 1.
[16] M. Abkowitz, J.S. Facci, M. Stolka, Chem. Phys. 177 (3) (1993) 783.
[17] P. Soustek, M. Michl, N. Almonasy, O. Machalicky, M. Dvorak, A. Lycka, Dyes Pigments 78 (2008) 139.
[18] M. Ozer, M. Kandaz, A.R. Ozkaya, M. Bulut, O. Guney, Dyes Pigments 76 (2008) 125.
[19] S. Alyar, N. Karacan, J. Enzym. Inhib. Med. Chem. 24 (2009) 986.
[20] S. Alyar, N. Ozbek, N. Karacan, Drug. Future 32 (2007) 125.
[21] N. Ozbek, S. Alyar, N. Karacan, Drug. Future 32 (2007) 27.
[22] A. Ienco, C. Mealli, P. Paoli, N. Dodoff, Z. Kantarci, N. Karacan, New J. Chem. 23 (1999) 1253.
[23] N.I. Dodoff, U. Ozdemir, N. Karacan, M.Ch. Georgieva, S.M. Konstantinov, M.E. Stefanova, Z. Naturforsch 54b (1999) 1553.
[24] S. Alyar, U.O. Ozmen, N. Karacan, O.S. Sentürk, K.A. Udachin, J. Mol. Struct. 889 (2008) 144.
[25] N. Ozbek, G. Kavak, Y. Ozcan, S. Ide, N. Karacan, J. Mol. Struct. 919 (2009) 154.
[26] U. Ozdemir Ozmen, G. Olgun, Spectrochim. Acta A 70 (2008) 641.
[27] G.G. Guilbault (Ed.), Practical Fluorescence, Marcel Dekker, New York, 1990.
[28] A. Gilbert, J. Bagott, Essentials of Molecular Photochemistry, CRC Press, Boca Raton Inc., Florida, 1991.
[29] (a) J.A. Osaheni, S.A. Jenekhe, J. Am. Chem. Soc. 117 (7) (1995) 7389;
(b) S.A. Jenekhe, J.A. Osaheni, Chem. Mater. 6 (1994) 1906.
[30] M.J. Frisch, G.W. Trucks, H.B.Schlegel, G.E. Scuseria, M.A.Robb, J.R. Cheeseman, J. A.Jr. Montgomery, T.Vreven, K.N. Kudin, J.C. Burant, J.M. Millam, S.S. Iyengar, J. Tomasi, V. Barone, B. Mennucci, M. Cossi, G. Scalmani, N. Rega, G.A. Petersson, H. Nakatsuji, M. Hada, M. Ehara, K. Toyota, R. Fukuda, J. Hasegawa, M. Ishida, T. Nakajima, Y. Honda, O. Kitao, H. Nakai, M. Klene, X. Li, J.E. Knox, H.P. Hratchian, J.B. Cross, C. Adamo, J. Jaramillo, R. Gomperts, R.E. Stratmann, O. Yazyev, A.J. Austin, R. Cammi, C. Pomelli, J.W. Ochterski, P.Y. Ayala, K. Morokuma, G.A. Voth, P. Salvador, J.J. Dannenberg, V.G. Zakrzewski, S. Dapprich, A.D. Daniels, M.C. Strain, O. Farkas, D.K. Malick, A.D. Rabuck, K. Raghavachari, J.B. Foresman, J.V. Ortiz, Q. Cui, A.G. Baboul, S. Clifford, J. Cioslowski, B.B. Stefanov, G. Liu, A. Liashenko, P. Piskorz, I. Komaromi, R.L. Martin, D.J. Fox, T. Keith, M.A. Al-Laham, C.Y. Peng, A. Nanayakkara, M. Challacombe, P.M.W. Gill, B. Johnson, W. Chen, M.W. Wong, C. Gonzalez, J.A. Pople, Gaussian 03, Revision B.04,Gaussian, Inc., Pittsburgh, PA, 2003.
[31] E.W. Koneman, S.D. Allen, W.M. Janda, P.C. Scherckenberger, W.C. Winn, Color Atlas and Textbook of Diagnostic Microbiology, Philadelphia, Lippincott-Raven, 1997.
[32] A.W. Bauer, W.M. Kirby, J.C. Sherris, M. Turck, Am. J. Clin. Pathol. 45 (1966) 493.
[33] N. Ozbek, S. Alyar, N. Karacan, J. Mol. Struct. 938 (2009) 48.
[34] N. Ozbek, H. Katırcıoglu, N. Karacan, T. Baykal, Bioorgan. Med. Chem 15 (2007) 5105.